

First observation of $\eta(1405)$ decays into $f_0(980)\pi^0$

M. Ablikim¹, M. N. Achasov⁵, D. Alberto⁴¹, D.J. Ambrose³⁸, F. F. An¹, Q. An³⁹, Z. H. An¹, J. Z. Bai¹, R. B. F. Baldini
 Ferrol¹⁷, Y. Ban²⁵, J. Becker², N. Berger¹, M. B. Bertani¹⁷, J. M. Bian¹, E. Boger^{18a}, O. Bondarenko¹⁹, I. Boyko¹⁸,
 R. A. Briere³, V. Bytev¹⁸, X. Cai¹, A. C. Calcaterra¹⁷, G. F. Cao¹, J. F. Chang¹, G. Chelkov^{18a}, G. Chen¹, H. S. Chen¹,
 J. C. Chen¹, M. L. Chen¹, S. J. Chen²³, Y. Chen¹, Y. B. Chen¹, H. P. Cheng¹³, Y. P. Chu¹, D. Cronin-Hennessy³⁷,
 H. L. Dai¹, J. P. Dai¹, D. Dedovich¹⁸, Z. Y. Deng¹, I. Denysenko^{18b}, M. Destefanis⁴¹, W. L. Ding Ding²⁷, Y. Ding²¹,
 L. Y. Dong¹, M. Y. Dong¹, S. X. Du⁴⁴, J. Fang¹, S. S. Fang¹, C. Q. Feng³⁹, C. D. Fu¹, J. L. Fu²³, Y. Gao³⁴, C. Geng³⁹,
 K. Goetzen⁷, W. X. Gong¹, M. Greco⁴¹, M. H. Gu¹, Y. T. Gu⁹, Y. H. Guan⁶, A. Q. Guo²⁴, L. B. Guo²², Y. P. Guo²⁴,
 Y. L. Han¹, X. Q. Hao¹, F. A. Harris³⁶, K. L. He¹, M. He¹, Z. Y. He²⁴, Y. K. Heng¹, Z. L. Hou¹, H. M. Hu¹, J. F. Hu⁶,
 T. Hu¹, B. Huang¹, G. M. Huang¹⁴, J. S. Huang¹¹, X. T. Huang²⁷, Y. P. Huang¹, T. Hussain⁴⁰, C. S. Ji³⁹, Q. Ji¹,
 X. B. Ji¹, X. L. Ji¹, L. K. Jia¹, L. L. Jiang¹, X. S. Jiang¹, J. B. Jiao²⁷, Z. Jiao¹³, D. P. Jin¹, S. Jin¹, F. F. Jing³⁴,
 N. Kalantar-Nayestanaki¹⁹, M. Kavatsyuk¹⁹, W. Kuehn³⁵, W. Lai¹, J. S. Lange³⁵, J. K. C. Leung³³, C. H. Li¹, Cheng Li³⁹,
 Cui Li³⁹, D. M. Li⁴⁴, F. Li¹, G. Li¹, H. B. Li¹, J. C. Li¹, K. Li¹⁰, Lei Li¹, N. B. Li²², Q. J. Li¹, S. L. Li¹, W. D. Li¹,
 W. G. Li¹, X. L. Li²⁷, X. N. Li¹, X. Q. Li²⁴, X. R. Li²⁶, Z. B. Li³¹, H. Liang³⁹, Y. F. Liang²⁹, Y. T. Liang³⁵, G. R. Liao³⁴,
 X. T. Liao¹, B. J. Liu³², C. L. Liu³, C. X. Liu¹, C. Y. Liu¹, F. H. Liu²⁸, Fang Liu¹, Feng Liu¹⁴, H. Liu¹, H. B. Liu⁶,
 H. H. Liu¹², H. M. Liu¹, H. W. Liu¹, J. P. Liu⁴², K. Liu²⁵, K. Liu⁶, K. Y. Liu²¹, Q. Liu³⁶, S. B. Liu³⁹, X. Liu²⁰, X. H. Liu¹,
 Y. B. Liu²⁴, Yong Liu¹, Z. A. Liu¹, Zhiqiang Liu¹, Zhiqing Liu¹, H. Loehner¹⁹, G. R. Lu¹¹, H. J. Lu¹³, J. G. Lu¹,
 Q. W. Lu²⁸, X. R. Lu⁶, Y. P. Lu¹, C. L. Luo²², M. X. Luo⁴³, T. Luo³⁶, X. L. Luo¹, M. Lv¹, C. L. Ma⁶, F. C. Ma²¹,
 H. L. Ma¹, Q. M. Ma¹, S. Ma¹, T. Ma¹, X. Y. Ma¹, M. Maggiora⁴¹, Q. A. Malik⁴⁰, H. Mao¹, Y. J. Mao²⁵, Z. P. Mao¹,
 J. G. Messchendorp¹⁹, J. Min¹, T. J. Min¹, R. E. Mitchell¹⁶, X. H. Mo¹, N. Yu. Muchnoi⁵, Y. Nefedov¹⁸, I. B. Nikolaev⁵,
 Z. Ning¹, S. L. Olsen²⁶, Q. Ouyang¹, S. P. Pacetti^{17c}, J. W. Park²⁶, M. Pelizaeus³⁶, K. Peters⁷, J. L. Ping²², R. G. Ping¹,
 R. Poling³⁷, C. S. J. Pun³³, M. Qi²³, S. Qian¹, C. F. Qiao⁶, X. S. Qin¹, J. F. Qiu¹, K. H. Rashid⁴⁰, G. Rong¹, X. D. Ruan⁹,
 A. Sarantsev^{18d}, J. Schulze², M. Shao³⁹, C. P. Shen^{36e}, X. Y. Shen¹, H. Y. Sheng¹, M. R. Shepherd¹⁶, X. Y. Song¹,
 S. Spataro⁴¹, B. Spruck³⁵, D. H. Sun¹, G. X. Sun¹, J. F. Sun¹¹, S. S. Sun¹, X. D. Sun¹, Y. J. Sun³⁹, Y. Z. Sun¹, Z. J. Sun¹,
 Z. T. Sun³⁹, C. J. Tang²⁹, X. Tang¹, E. H. Thorndike³⁸, H. L. Tian¹, D. Toth³⁷, G. S. Varner³⁶, X. Wan¹, B. Wang⁹,
 B. Q. Wang²⁵, K. Wang¹, L. L. Wang⁴, L. S. Wang¹, M. Wang²⁷, P. Wang¹, P. L. Wang¹, Q. Wang¹, Q. J. Wang¹,
 S. G. Wang²⁵, X. F. Wang¹¹, X. L. Wang³⁹, Y. D. Wang³⁹, Y. F. Wang¹, Y. Q. Wang²⁷, Z. Wang¹, Z. G. Wang¹,
 Z. Y. Wang¹, D. H. Wei⁸, Q. G. Wen³⁹, S. P. Wen¹, U. Wiedner², L. H. Wu¹, N. Wu¹, W. Wu²⁴, Z. Wu¹, Z. J. Xiao²²,
 Y. G. Xie¹, Q. L. Xiu¹, G. F. Xu¹, G. M. Xu²⁵, H. Xu¹, Q. J. Xu¹⁰, X. P. Xu³⁰, Y. Xu²⁴, Z. R. Xu³⁹, Z. Xue¹, L. Yan³⁹,
 W. B. Yan³⁹, Y. H. Yan¹⁵, H. X. Yang¹, T. Yang⁹, Y. Yang¹⁴, Y. X. Yang⁸, H. Ye¹, M. Ye¹, M. H. Ye⁴, B. X. Yu¹,
 C. X. Yu²⁴, S. P. Yu²⁷, C. Z. Yuan¹, W. L. Yuan²², Y. Yuan¹, A. A. Zafar⁴⁰, A. Z. Zallo¹⁷, Y. Zeng¹⁵, B. X. Zhang¹,
 B. Y. Zhang¹, C. C. Zhang¹, D. H. Zhang¹, H. H. Zhang³¹, H. Y. Zhang¹, J. Zhang²², J. Q. Zhang¹, J. W. Zhang¹,
 J. Y. Zhang¹, J. Z. Zhang¹, L. Zhang²³, S. H. Zhang¹, T. R. Zhang²², X. J. Zhang¹, X. Y. Zhang²⁷, Y. Zhang¹,
 Y. H. Zhang¹, Y. S. Zhang⁹, Z. P. Zhang³⁹, Z. Y. Zhang⁴², G. Zhao¹, H. S. Zhao¹, Jingwei Zhao¹, Lei Zhao³⁹, Ling Zhao¹,
 M. G. Zhao²⁴, Q. Zhao¹, S. J. Zhao⁴⁴, T. C. Zhao¹, X. H. Zhao²³, Y. B. Zhao¹, Z. G. Zhao³⁹, A. Zhemchugov^{18a}, B. Zheng¹,
 J. P. Zheng¹, Y. H. Zheng⁶, Z. P. Zheng¹, B. Zhong¹, J. Zhong², L. Zhou¹, X. K. Zhou⁶, X. R. Zhou³⁹, C. Zhu¹, K. Zhu¹,
 K. J. Zhu¹, S. H. Zhu¹, X. L. Zhu³⁴, X. W. Zhu¹, Y. S. Zhu¹, Z. A. Zhu¹, J. Zhuang¹, B. S. Zou¹, J. H. Zou¹, J. X. Zuo¹

(BESIII Collaboration)

¹ Institute of High Energy Physics, Beijing 100049, P. R. China

² Bochum Ruhr-University, 44780 Bochum, Germany

³ Carnegie Mellon University, Pittsburgh, PA 15213, USA

⁴ China Center of Advanced Science and Technology, Beijing 100190, P. R. China

⁵ G.I. Budker Institute of Nuclear Physics SB RAS (BINP), Novosibirsk 630090, Russia

⁶ Graduate University of Chinese Academy of Sciences, Beijing 100049, P. R. China

⁷ GSI Helmholtzcentre for Heavy Ion Research GmbH, D-64291 Darmstadt, Germany

⁸ Guangxi Normal University, Guilin 541004, P. R. China

⁹ Guangxi University, Nanning 530004, P. R. China

¹⁰ Hangzhou Normal University, XueLin Jie 16, XiaSha Higher Education Zone, Hangzhou, 310036

¹¹ Henan Normal University, Xinxiang 453007, P. R. China

¹² Henan University of Science and Technology,

¹³ Huangshan College, Huangshan 245000, P. R. China

¹⁴ Huazhong Normal University, Wuhan 430079, P. R. China

¹⁵ Hunan University, Changsha 410082, P. R. China

¹⁶ Indiana University, Bloomington, Indiana 47405, USA

¹⁷ INFN Laboratori Nazionali di Frascati, Frascati, Italy

¹⁸ Joint Institute for Nuclear Research, 141980 Dubna, Russia

¹⁹ KVI/University of Groningen, 9747 AA Groningen, The Netherlands

²⁰ Lanzhou University, Lanzhou 730000, P. R. China

²¹ Liaoning University, Shenyang 110036, P. R. China

²² Nanjing Normal University, Nanjing 210046, P. R. China

²³ Nanjing University, Nanjing 210093, P. R. China

- ²⁴ Nankai University, Tianjin 300071, P. R. China
²⁵ Peking University, Beijing 100871, P. R. China
²⁶ Seoul National University, Seoul, 151-747 Korea
²⁷ Shandong University, Jinan 250100, P. R. China
²⁸ Shanxi University, Taiyuan 030006, P. R. China
²⁹ Sichuan University, Chengdu 610064, P. R. China
³⁰ Soochow University, Suzhou 215006, China
³¹ Sun Yat-Sen University, Guangzhou 510275, P. R. China
³² The Chinese University of Hong Kong, Shatin, N.T., Hong Kong.
³³ The University of Hong Kong, Pokfulam, Hong Kong
³⁴ Tsinghua University, Beijing 100084, P. R. China
³⁵ Universitaet Giessen, 35392 Giessen, Germany
³⁶ University of Hawaii, Honolulu, Hawaii 96822, USA
³⁷ University of Minnesota, Minneapolis, MN 55455, USA
³⁸ University of Rochester, Rochester, New York 14627, USA
³⁹ University of Science and Technology of China, Hefei 230026, P. R. China
⁴⁰ University of the Punjab, Lahore-54590, Pakistan
⁴¹ University of Turin and INFN, Turin, Italy
⁴² Wuhan University, Wuhan 430072, P. R. China
⁴³ Zhejiang University, Hangzhou 310027, P. R. China
⁴⁴ Zhengzhou University, Zhengzhou 450001, P. R. China
- ^a also at the Moscow Institute of Physics and Technology, Moscow, Russia
^b on leave from the Bogolyubov Institute for Theoretical Physics, Kiev, Ukraine
^c Currently at University of Perugia and INFN, Perugia, Italy
^d also at the PNPI, Gatchina, Russia
^e now at Nagoya University, Nagoya, Japan

The decays $J/\psi \rightarrow \gamma\pi^+\pi^-\pi^0$ and $J/\psi \rightarrow \gamma\pi^0\pi^0\pi^0$ are analyzed using a sample of 225 million J/ψ events collected with the BESIII detector. The isospin violating decay $\eta(1405) \rightarrow f_0(980)\pi^0$ with $f_0(980) \rightarrow \pi^+\pi^-(\pi^0\pi^0)$ is observed for the first time. The width of the $f_0(980)$ observed in the dipion mass spectra is much narrower than the world average. Decay rates for three-pion decays of the η' are also measured precisely.

PACS numbers: 14.40.Be, 12.38.Qk, 13.25.Gv

A state near 1440 MeV/ c^2 was discovered in $p\bar{p}$ annihilation at rest decaying to $\eta\pi^+\pi^-$ and was subsequently observed decaying to $K\bar{K}\pi$ [1]. Considerable theoretical and experimental efforts have since been devoted to understand its nature. It was proposed to be a candidate for a pseudo-scalar glueball [2, 3]; the measured mass, however, is much lower than that obtained from lattice QCD calculations, which is above 2 GeV/ c^2 [4]. Later, experiments produced evidence that this state was really two different pseudo-scalar states, the $\eta(1405)$ and the $\eta(1475)$. The former has large couplings to $a_0(980)\pi$ and $K\bar{K}\pi$, while the latter mainly couples to $K^*\bar{K}$. A detailed review of the experimental situation can be found in Ref. [5].

The nature of the well-established light scalars $f_0(980)$ and $a_0(980)$ is also a matter of controversy. It is not clear whether they belong to the light scalar meson nonet or are examples of mesons beyond the naive quark model (eg. tetra-quark states, hybrids or $K\bar{K}$ molecules) [6–11]. The possibility of mixing between the $f_0(980)$ and $a_0^0(980)$ was suggested long ago, and its measurement sheds light on the nature of these two resonances [12–17].

The three-pion decays of the η' have garnered attention because their branching ratios (Br) can probe isospin breaking [18, 19]. The ratios of the branching ratios

($r_{\pm} \equiv Br(\eta' \rightarrow \pi^+\pi^-\pi^0)/Br(\eta' \rightarrow \pi^+\pi^-\eta)$ and $r_0 \equiv Br(\eta' \rightarrow 3\pi^0)/Br(\eta' \rightarrow \pi^0\pi^0\eta)$) are related to the strange quark mass and SU(3) breaking [18].

In this letter, we present the results of a study of $J/\psi \rightarrow \gamma\pi^+\pi^-\pi^0$ and $J/\psi \rightarrow \gamma\pi^0\pi^0\pi^0$. A single structure around 1.4 GeV/ c^2 in the $\pi^+\pi^-\pi^0$ ($\pi^0\pi^0\pi^0$) mass spectrum is observed, associated with a narrow structure around 980 MeV/ c^2 in the $\pi^+\pi^-(\pi^0\pi^0)$ mass spectrum. This analysis is based on a sample of $(225.2 \pm 2.8) \times 10^6$ J/ψ events [20] accumulated in the Beijing Spectrometer (BESIII) [21] operating at the Beijing Electron-Positron Collider (BEPCII) [22].

BEPCII is a double-ring e^+e^- collider designed to provide e^+e^- collisions with a peak luminosity of 10^{33} cm $^{-2}$ s $^{-1}$ at a beam current of 0.93 A. The cylindrical core of the BESIII detector consists of a helium-based main drift chamber (MDC), a plastic scintillator time-of-flight system (TOF), and a CsI(Tl) electromagnetic calorimeter (EMC), which are all enclosed in a superconducting solenoidal magnet providing a 1.0 T magnetic field. The solenoid is supported by an octagonal flux-return yoke with resistive plate counter muon identifier modules interleaved with steel. The acceptance of charged particles and photons is 93% over 4π stereo angle, and the charged-particle

momentum and photon energy resolutions at 1 GeV are 0.5% and 2.5%, respectively. The BESIII detector is modeled with a Monte Carlo (MC) simulation based on GEANT4 [23, 24].

The charged-particle tracks in the polar angle range $|\cos\theta| < 0.93$ are reconstructed from hits in the MDC. Tracks that extrapolate to be within 20 cm of the interaction point in the beam direction and 2 cm in the plane perpendicular to the beam are selected. The TOF and dE/dx information are combined to form particle identification confidence levels for the π , K , and p hypotheses; each track is assigned to the particle type that corresponds to the hypothesis with the highest confidence level. Photon candidates are required to have at least 25 MeV and 50 MeV of energy in the EMC regions $|\cos\theta| < 0.8$ and $0.86 < |\cos\theta| < 0.92$, respectively, and be separated from all charged tracks by more than 10° .

For $J/\psi \rightarrow \gamma\pi^+\pi^-\pi^0$, the candidate events are required to have two oppositely charged tracks identified as pions and at least three photon candidates. A four-constraint(4C) energy-momentum conserving kinematic fit is performed to the $\gamma\gamma\gamma\pi^+\pi^-$ hypothesis, and $\chi^2_{4C} < 30$ is required. For events with more than three photon candidates, the combination with the smallest χ^2 is retained. To reject possible background events with two or four photons in the final state, the 4C-fit probability for an assignment of the $J/\psi \rightarrow \pi^+\pi^-\gamma\gamma\gamma$ channel must be larger than that of the $J/\psi \rightarrow \pi^+\pi^-\gamma\gamma$ and the $J/\psi \rightarrow \pi^+\pi^-\gamma\gamma\gamma\gamma$ channels. The π^0 candidates are selected by requiring $|M_{\gamma\gamma} - m_{\pi^0}| < 0.015 \text{ GeV}/c^2$. Events with $|M_{\gamma\pi^0} - m_\omega| < 0.05 \text{ GeV}/c^2$ are rejected to suppress the background from $J/\psi \rightarrow \omega\pi^+\pi^-$.

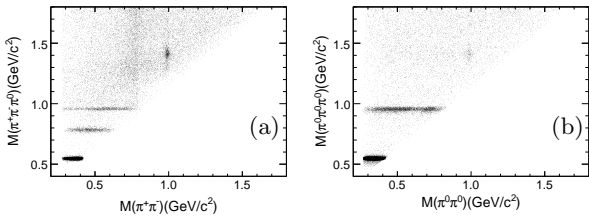


FIG. 1: (a) Scatter plot of $M_{\pi^+\pi^-\pi^0}$ versus $M_{\pi^+\pi^-}$. (b) Scatter plot of $M_{\pi^0\pi^0\pi^0}$ versus $M_{\pi^0\pi^0}$ (3 entries per event).

For $J/\psi \rightarrow \gamma 3\pi^0$, the candidate events are required to have no charged track. The $\pi^0 \rightarrow \gamma\gamma$ candidates are formed from pairs of photon candidates that are kinematically fit to the π^0 mass, and the χ^2 from the kinematic fit with 1 degree of freedom are required to be less than 25. True π^0 mesons decay isotropically in the π^0 rest frame, and their decay distributions are flat, contrary to π^0 candidates originating from wrong photon combinations. To remove wrong photon combinations, the decay angle, defined as the polar angle of a photon in the π^0 rest frame, is required to satisfy $|\cos\theta_{decay}| < 0.95$. Events with at least seven

and less than nine photons, which form at least three distinct π^0 candidates, are selected. A 7C kinematic fit is performed to the $J/\psi \rightarrow \gamma 3\pi^0$ hypothesis (constraints are the 4-momentum of J/ψ and the three π^0 masses), and $\chi^2_{7C} < 60$ is required. If there is more than one combination, the combination with the smallest χ^2_{7C} is retained. Events with $|M_{\gamma\pi^0} - m_\omega| < 0.05 \text{ GeV}/c^2$ are rejected to suppress the background from $J/\psi \rightarrow \omega\pi^0\pi^0$.

The distributions of the selected events in the $M_{\pi^+\pi^-\pi^0}$ - $M_{\pi^+\pi^-}$ and $M_{\pi^0\pi^0\pi^0}$ - $M_{\pi^0\pi^0}$ planes are shown in Fig. 1 (a) and (b), respectively. The clusters corresponding to $\eta \rightarrow 3\pi$, $\eta' \rightarrow 3\pi$ and $\eta(1405) \rightarrow f_0(980)\pi^0$ can be clearly discerned; the ω signal is also evident in Fig. 1 (a), which mainly comes from the background channel $J/\psi \rightarrow \omega\pi^0$, while it is not observed in the neutral channel, as expected from charge conjugation symmetry.

To confirm that the apparent signal for $\eta(1405) \rightarrow f_0(980)\pi^0$ is not caused by background events, we perform a study with an inclusive MC sample of 2.25×10^8 J/ψ events generated according to the Lund-Charm model [25] and the Particle Data Group (PDG) decay tables [26]. After the same event selection as above, neither $\eta(1405)$ nor $f_0(980)$ are seen in the mass spectra. Non- $f_0(980)$ or non- $\eta(1405)$ processes are studied using the $f_0(980)$ sidebands ($0.88 \text{ GeV}/c^2 < M_{\pi^+\pi^-(\pi^0\pi^0)} < 0.93 \text{ GeV}/c^2$ and $1.05 \text{ GeV}/c^2 < M_{\pi^+\pi^-(\pi^0\pi^0)} < 1.10 \text{ GeV}/c^2$) or the $\eta(1405)$ sidebands ($1.15 \text{ GeV}/c^2 < M_{\pi^+\pi^-\pi^0(\pi^0\pi^0\pi^0)} < 1.25 \text{ GeV}/c^2$ and $1.55 \text{ GeV}/c^2 < M_{\pi^+\pi^-\pi^0(\pi^0\pi^0\pi^0)} < 1.65 \text{ GeV}/c^2$). No peaking structures are observed.

Fig. 2 (a) and (b) show the $\pi^+\pi^-$ and $\pi^0\pi^0$ mass spectra with the requirement $1.3 \text{ GeV}/c^2 < M_{\pi^+\pi^-\pi^0(3\pi^0)} < 1.5 \text{ GeV}/c^2$. A fit is performed to the $\pi^+\pi^-$ mass spectrum with the $f_0(980)$ signal parameterized by a Breit-Wigner function convolved with a Gaussian mass resolution function plus a second-order Chebychev polynomial background function. The mass, width and number of events of the $f_0(980)$ obtained from the fit are $m = 989.9 \pm 0.4 \text{ MeV}/c^2$, $\Gamma = 9.5 \pm 1.1 \text{ MeV}/c^2$ and $N = 706 \pm 41$, respectively. A fit to the $\pi^0\pi^0$ mass spectrum, shown in Fig. 2 (b), is performed in a similar fashion. The mass, width and number of events of the $f_0(980)$ obtained from the fit are $m = 987.0 \pm 1.4 \text{ MeV}/c^2$, $\Gamma = 4.6 \pm 5.1 \text{ MeV}/c^2$ and $N = 190 \pm 30$, respectively. The measured width of the $f_0(980)$ is much narrower than the world average.

Figs. 3 (a) and (b) show the $\pi^+\pi^-\pi^0$ and $\pi^0\pi^0\pi^0$ mass spectra where $\pi^+\pi^-(\pi^0\pi^0)$ is in the $f_0(980)$ mass region ($0.94 \text{ GeV}/c^2 < M_{\pi^+\pi^-(\pi^0\pi^0)} < 1.04 \text{ GeV}/c^2$). In addition to the $\eta(1405)$, there is an enhancement at $1.3 \text{ GeV}/c^2$. A fit is performed to the $\pi^+\pi^-\pi^0$ mass spectrum. The two peaks are parameterized by efficiency-corrected Breit-Wigner functions convolved with a Gaussian resolution function. The mass and width of the small enhancement are fixed to PDG values of $f_1(1285)$ [26]. The background is described by a third-order Chebychev polynomial with shape

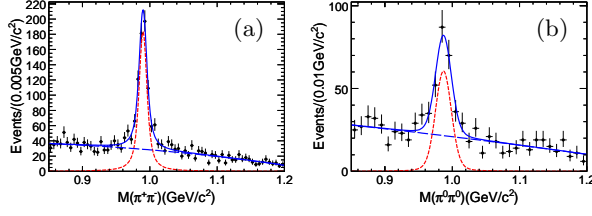


FIG. 2: The $\pi^+\pi^-$ and $\pi^0\pi^0$ invariant mass spectra with $\pi^+\pi^-\pi^0(3\pi^0)$ in the $\eta(1405)$ mass region. The solid curve is the result of the fit described in the text. The dotted curve is the $f_0(980)$ signal. The dashed curve denotes the background polynomial.

parameters determined from a simultaneous fit to the $\pi^+\pi^-\pi^0$ mass spectrum while the $\pi^+\pi^-$ invariant mass is found in the $f_0(980)$ sidebands. The normalization of each component is allowed to float. The masses, widths, number of events, efficiencies, and the product branching ratios of the $\eta(1405)$ and the possible $f_1(1285)/\eta(1295)$ contribution are listed in Table I. The statistical significance of the $\eta(1405)$ is determined by the change of the fit likelihood $-2\ln L$ obtained from the fits with and without the assumption of the $\eta(1405)$ and is found to be well above 10σ . The significance of the potential $f_1(1285)/\eta(1295)$ contribution is determined to be 3.7σ . A fit to the $\pi^0\pi^0\pi^0$ mass spectrum is performed in a similar fashion, shown in Fig. 3 (b). The significance of the $\eta(1405)$ is determined to be larger than 10σ . For a possible $f_1(1285)/\eta(1295)$ contribution, the significance is only 1.2σ , and we derive an upper limit on the branching ratio at the 90% C.L. using the Bayesian method.

An angular-distribution analysis is performed with the selected $J/\psi \rightarrow \gamma\eta(1405) \rightarrow \gamma f_0(980)\pi^0 \rightarrow \gamma\pi^+\pi^-\pi^0$ events. Backgrounds are subtracted using the $f_0(980)$ sideband events. For radiative J/ψ decays to a $J^P = 0^-$ meson, the polar angle θ_γ of the photon in the J/ψ center-of-mass system should be distributed according to $1 + \cos^2\theta_\gamma$. In the case of a $J^P = 1^+$ meson, the distributions $\frac{d\sigma}{d\cos\theta_\gamma} \sim 1 + 2|\alpha|^2 + (1 - 2|\alpha|^2)\cos^2\theta_\gamma$ and $\frac{d\sigma}{d\cos\theta_{f_0(980)}} \sim 2 + (|\alpha|^2 - 2)\sin^2\theta_{f_0(980)}$ are expected, where $\theta_{f_0(980)}$ is the polar angle of $f_0(980)$ in the helicity frame of $\eta(1405)$, α is the ratio of helicity 1 to helicity 0. For the $J^P = 1^+$ assumption, $|\alpha|^2$ is determined to be 2.10 ± 0.26 from a fit to $\cos\theta_{f_0(980)}$ (Fig. 3 (c)). The fitting $\chi^2/n.d.f.$ of Fig. 3 (d) with $|\alpha|^2 = 2.10$ is 59.4/15. For the $J^P = 0^-$ assumption, the fitting $\chi^2/n.d.f.$ of Fig. 3 (d) is 38.4/15. The fitting results favor the $J^P = 0^-$ assignment of the $\eta(1405)$.

Figs. 4 (a) and (b) show the $\pi^+\pi^-\pi^0$ and $\pi^0\pi^0\pi^0$ mass spectra in the η' region. A fit is performed to the $\pi^+\pi^-\pi^0$ mass spectrum, shown in Fig. 4 (a). The shape of the η' is obtained from MC simulation and the mass and width of the η' are fixed to its PDG values [26]. The shape of the peaking backgrounds ($J/\psi \rightarrow \gamma\eta' \rightarrow \gamma\gamma\rho^0(\pi^+\pi^-)$ and $J/\psi \rightarrow \gamma\eta' \rightarrow \gamma\gamma\omega(\pi^+\pi^-\pi^0)$) are from exclusive

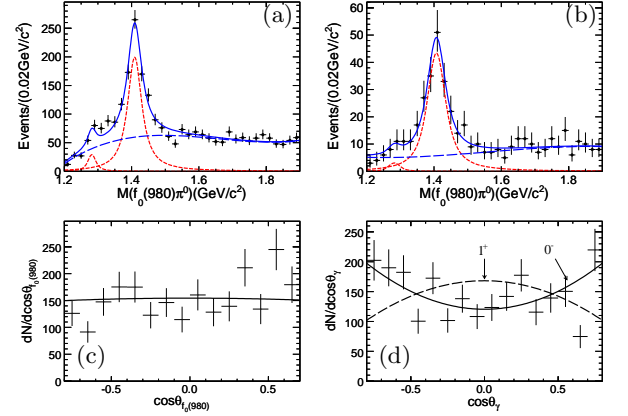


FIG. 3: Results of the fit to (a) the $f_0(980)(\pi^+\pi^-)\pi^0$ and (b) $f_0(980)(\pi^0\pi^0)\pi^0$ invariant mass spectra. The solid curve is the result of the fit described in the text. The dotted curve is the $f_1(1285)/\eta(1295)$ and $\eta(1405)$ signal. The dashed curves denote the background polynomial. Angular distributions of the signal include efficiency corrections. (c) The $\cos\theta_{f_0(980)}$ distribution. The fitting result of $\cos\theta_{f_0(980)}$ is $|\alpha|^2 = 2.10 \pm 0.26$. (d) The $\cos\theta_\gamma$ distribution. The solid line is the prediction for the $J^P = 0^-$ hypothesis, and the dashed line is the prediction for the $J^P = 1^+$ hypothesis with $|\alpha|^2 = 2.10$.

MC samples with predicted background levels of 361 ± 32 and 32 ± 6 events, normalized by branching ratios in the PDG [26] and fixed in the fit. The error on the number of events is estimated by changing the normalization by one standard deviation from the PDG value. A second-order Chebychev polynomial is used to describe the sum of other non-peaking backgrounds. For $\eta' \rightarrow \pi^0\pi^0\pi^0$, $\chi^2(\gamma\pi^0\pi^0\pi^0) < \chi^2(\gamma\eta\pi^0\pi^0)$ and $|M_{\gamma\gamma} - m_{\eta}| > 0.03$ GeV/ c^2 are additionally required to remove background events from $\eta' \rightarrow \eta\pi^0\pi^0$. A fit to the $\pi^0\pi^0\pi^0$ mass spectrum is performed as shown in Fig. 4 (b). The shapes of the η' and non-peaking backgrounds are described analogously to the charged mode. The efficiencies and the product branching ratios for the η' obtained from the fit are also listed in Table I. From our measurement and the world average values for branching ratios of $\eta' \rightarrow \eta\pi\pi$ [26], we determine $r_\pm = (8.87 \pm 0.98) \times 10^{-3}$ and $r_0 = (16.41 \pm 1.94) \times 10^{-3}$.

The systematic uncertainties on the signal yield arise from fit ranges, signal shapes and background estimation. In detail, for the $\eta(1405)$ signal, the signal shape is given by a Breit-Wigner function with floating mass and width. Its uncertainties are estimated by fixing the mass and width of the $\eta(1405)$ to the world average values. For the possible $f_1(1285)/\eta(1295)$ contribution and η' signal, uncertainties are estimated by changing their mass and width by one standard deviation from the PDG values. The uncertainty due to the assumed background shape for the $\eta(1405)$ and the $f_1(1285)/\eta(1295)$ has been estimated using different $f_0(980)$ sidebands; while that of the η' is studied using

TABLE I: Summary of measurements of the masses, widths, number of events, the MC efficiencies(ϵ) and the product branching ratios of $Br(J/\psi \rightarrow \gamma X) \times Br(X \rightarrow \pi^0 f_0(980)) \times Br(f_0(980) \rightarrow \pi\pi)$ and the decay branching ratios of $Br(Y \rightarrow 3\pi)$ for the $\pi^+\pi^-\pi^0$ and $\pi^0\pi^0\pi^0$ channels, where X represents $\eta(1405)$ and the possible $f_1(1285)/\eta(1295)$ contribution, Y represents η' . Here for the branching ratios, the first errors are statistical and the second ones are systematic.

Resonance	M(MeV/c ²)	Γ (MeV/c ²)	N_{event}	ϵ (%)	Branching ratios
$\eta(1405)(\pi^+\pi^-\pi^0)$	1409.0 ± 1.7	48.3 ± 5.2	743 ± 56	22.20	$(1.50 \pm 0.11 \pm 0.11) \times 10^{-5}$
$\eta(1405)(\pi^0\pi^0\pi^0)$	1407.0 ± 3.5	55.0 ± 11.0	198 ± 23	12.83	$(7.10 \pm 0.82 \pm 0.72) \times 10^{-6}$
$f_1(1285)/\eta(1295)(\pi^+\pi^-\pi^0)$	fixed	fixed	60 ± 18	26.99	$(9.99 \pm 3.00 \pm 1.03) \times 10^{-7}$
$f_1(1285)/\eta(1295)(\pi^0\pi^0\pi^0)$	fixed	fixed	23	16.75	$< 7.11 \times 10^{-7}$
$\eta'(\pi^+\pi^-\pi^0)$	fixed	fixed	1014 ± 39	22.52	$(3.83 \pm 0.15 \pm 0.39) \times 10^{-3}$
$\eta'(\pi^0\pi^0\pi^0)$	fixed	fixed	309 ± 19	7.57	$(3.56 \pm 0.22 \pm 0.34) \times 10^{-3}$

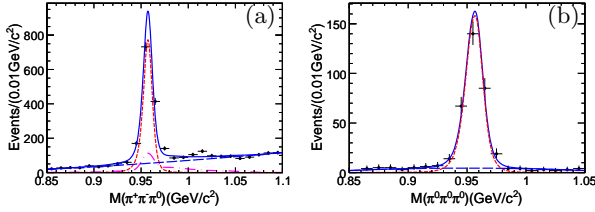


FIG. 4: Results of the fit to (a) the $\pi^+\pi^-\pi^0$ and (b) $3\pi^0$ invariant mass spectra. The solid curve is the result of the fit described in the text. The dotted curve is the η' signal. The dashed curves denote the background polynomial. The dash-dotted curve in (a) describes the peaking background.

different order polynomials. For $\eta' \rightarrow \pi^+\pi^-\pi^0$, the uncertainty of the peaking background is estimated by using the shape from the π^0 sidebands instead of using the shape from exclusive MC samples. The systematic errors on the branching ratio measurements are also subject to systematic uncertainties in the number of J/ψ events [20], the intermediate branching ratios [26], the data-MC difference in the π tracking efficiency, the photon detection efficiency, particle identification, the kinematic fit and the π^0 selection. Combined in quadrature with the uncertainty from the mass spectrum fitting, the systematic errors on the product branching ratios of the $\eta(1405)$, $f_1(1285)/\eta(1295)$ and η' are summarized in Table I.

The $\eta(1405) \rightarrow f_0(980)\pi^0$ signal could arise via $a_0^0(980) - f_0(980)$ mixing. Using the branching ratio of $J/\psi \rightarrow \gamma\eta(1405) \rightarrow \gamma\eta\pi^+\pi^-$ [26] and the largest PDG value of $\Gamma(\eta(1405) \rightarrow a_0(980)\pi)/\Gamma(\eta(1405) \rightarrow \eta\pi\pi)$ [27], $Br(J/\psi \rightarrow \gamma\eta(1405) \rightarrow \gamma a_0^0(980)\pi^0 \rightarrow \gamma\pi^0\eta\pi^0) = (8.40 \pm 1.75) \times 10^{-5}$. The $a_0^0(980) - f_0(980)$ mixing intensity measured from the process $\chi_{c1} \rightarrow a_0^0(980)\pi^0 \rightarrow f_0(980)\pi^0 \rightarrow \pi^+\pi^-\pi^0$ at BES III is less than 1% (90% C.L.) [28]. The branching ratio of $J/\psi \rightarrow \gamma\eta(1405) \rightarrow \gamma a_0^0(980)\pi^0 \rightarrow \gamma f_0(980)\pi^0 \rightarrow \gamma\pi^+\pi^-\pi^0$ is thus expected to be less than $(8.40 \pm 1.75) \times 10^{-7}$, which is much smaller than the result that we measure. Therefore, $a_0^0(980) - f_0(980)$ mixing alone can not explain the observed branching ratio of $\eta(1405) \rightarrow f_0(980)\pi^0$.

In the triangle singularity scenario, recently introduced by J.J. Wu et al. [29], only one 0^{-+} isoscalar is

needed in the vicinity of 1.44 GeV/c². Interferences from the triangle singularity can shift the peak position to a lower value. According to this mechanism, the decay $\eta(1405) \rightarrow f_0(980)\pi^0$ dominantly comes from an intermediate on-shell $K\bar{K}^* + c.c.$ pair by exchanging an on-shell kaon, and the narrow width is caused by the non-perfect cancellation between the charged and neutral $K\bar{K}^*(K)$ loops due to the mass difference between charged and neutral kaons. Further study is needed to understand this anomalously large isospin violating decay.

In summary, we have studied $J/\psi \rightarrow \gamma 3\pi$ decays. The isospin violating decay $\eta(1405) \rightarrow f_0(980)\pi^0$ is observed for the first time with a statistical significance larger than 10σ in both the charged and neutral modes. According to our measurement, the ratio of $Br(\eta(1405) \rightarrow f_0(980)\pi^0 \rightarrow \pi^+\pi^-\pi^0)$ to $Br(\eta(1405) \rightarrow a_0^0(980)\pi^0 \rightarrow \eta\pi^0\pi^0)$ is $(17.9 \pm 4.2)\%$ [26, 27], which is one order of magnitude larger than the $a_0^0(980) - f_0(980)$ mixing intensity (less than 1%) determined at BESIII previously [28]. There is also evidence for an enhancement at around 1.3 GeV/c² (potentially from the $f_1(1285)/\eta(1295)$) seen with a significance of 3.7σ in the charged mode and 1.2σ in the neutral mode. For the decay $\eta' \rightarrow \pi^+\pi^-\pi^0$, the branching ratio that we measure is consistent with the CLEO-c measurement [30], and the precision is improved by a factor of four. For the decay $\eta' \rightarrow 3\pi^0$, it is two times larger than the world average value [26]. Using our new measurement of the decay rates for $\eta' \rightarrow 3\pi$, the values of r_{\pm} and r_0 are not consistent with the π^0 - η mixing prediction, nor with the chiral unitary framework prediction [19].

The BESIII collaboration thanks the staff of BEPCII and the computing center for their hard efforts. Useful discussions with K.T. Chao, S.L. Zhu, and J.J. Wu are acknowledged. This work is supported in part by the Ministry of Science and Technology of China under Contract No. 2009CB825200; National Natural Science Foundation of China (NSFC) under Contracts Nos. 10625524, 10821063, 10825524, 10835001, 10935007, 11125525; the Chinese Academy of Sciences (CAS) Large-Scale Scientific Facility Program; CAS under Contracts Nos. KJCX2-YW-N29, KJCX2-YW-N45; 100 Talents Program of CAS; Istituto Nazionale di Fisica Nucleare, Italy; Siberian Branch of Russian Academy of

Science, joint project No 32 with CAS; U. S. Department of Energy under Contracts Nos. DE-FG02-04ER41291, DE-FG02-91ER40682, DE-FG02-94ER40823; University of Groningen (RuG) and the Helmholtzzentrum fuer

Schwerionenforschung GmbH (GSI), Darmstadt; WCU Program of National Research Foundation of Korea under Contract No. R32-2008-000-10155-0.

-
- [1] P.H. Baillon *et al.*, Nuovo Cimento **50A**, 393 (1967).
 - [2] M. Acciarri *et al.* (L3 Collaboration), Phys. Lett. B **501**, 1 (2001).
 - [3] L. Faddeev *et al.*, Phys. Rev. D **70**, 114033 (2004).
 - [4] G. S. Bali *et al.*, Phys. Lett. B **309**, 378 (1993).
 - [5] A. Masoni, C. Cicalo, and G.L. Usai, J. Phys. **G32**, R293 (2006).
 - [6] R. L. Jaffe, Phys. Rev. D **15**, 267 (1977).
 - [7] N. N. Achasov and V. N. Ivanchenko, Nucl. Phys. B **315**, 465 (1989).
 - [8] N. N. Achasov and V.V. Gubin, Phys. Rev. D **56**, 4084 (1997).
 - [9] J. D. Weinstein and N. Isgur, Phys. Rev. D **27**, 588 (1983).
 - [10] J. D. Weinstein and N. Isgur, Phys. Rev. D **41**, 2236 (1990).
 - [11] S. Ishida *et al.*, in Proceedings of the 6th International Conference on Hadron Spectroscopy, Manchester, United Kingdom, 1995 (World Scientific, Singapore, 1995), p. 454.
 - [12] N. N. Achasov, S. A. Devyanin and G. N. Shestakov, Phys. Lett. B **88**, 367 (1979).
 - [13] C. Hanhart, B. Kubis and J. R. Pelaez, Phys. Rev. D **76**, 074028 (2007).
 - [14] N. N. Achasov and A. V. Kiselev, Phys. Lett. B **534**, 83 (2002).
 - [15] B. Kerbikov and F. Tabakin, Phys. Rev. C **62**, 064601 (2000).
 - [16] N. N. Achasov and G. N. Shestakov, Phys. Rev. Lett. **92**, 182001 (2004).
 - [17] F. E. Close and A. Kirk, Phys. Lett. B **489**, 24 (2000).
 - [18] D.J. Gross, S.B. Treiman, and F. Wilczek, Phys. Rev. D **19**, 2188(1979).
 - [19] B. Borasoy, U.-G. Meissner, and R. Nissler, Phys. Lett. B **643**, 41(2006).
 - [20] M. Ablikim *et al.* (BESIII Collaboration), Phys. Rev. D **83**, 012003 (2011).
 - [21] M. Ablikim *et al.* (BESIII Collaboration), Nucl. Instrum. Methods Phys. Res., Sect. A **614**, 345 (2010).
 - [22] J. Z. Bai *et al.* (BES Collaboration), Nucl. Instrum. Methods Phys. Res. A **458**, 627 (2001).
 - [23] S. Agostinelli *et al.* (GEANT4 Collaboration), Nucl. Instrum. Methods Phys. Res. A **506**, 250 (2003).
 - [24] J. Allison *et al.*, IEEE Trans. Nucl. Sci. **53**, 270 (2006).
 - [25] R. G. Ping, Chinese Phys. C **32**, 599 (2008).
 - [26] K. Nakamura *et al.* (Particle Data Group), J. Phys. G **37**, 075021 (2010).
 - [27] C. Amsler *et al.* (Crystal Barrel Collaboration), Phys. Lett. B **358**, 389 (1995).
 - [28] M. Ablikim *et al.* (BESIII Collaboration), Phys. Rev. D **83**, 032003 (2011).
 - [29] J.J. Wu *et al.*, e-Print Archive:arXiv:1108.3772[hep-ex]
 - [30] P. Naik *et al.* (CLEO Collaboration), Phys. Rev. Lett. **102**, 061801 (2009).